Langmuir

Article

pubs.acs.org/Langmuir

Decontamination of Bisphenol A from Aqueous Solution by Graphene Adsorption

Jing Xu,[†] Li Wang,[†] and Yongfa Zhu[†,‡,*]

[†]Department of Chemistry, Tsinghua University, Beijing 100084, China

[‡]Jiangsu Key Laboratory of Atmospheric Environment Monitoring and Pollution Control, Nanjing University of Information Science and Technology, Nanjing 210044, China

Supporting Information

ABSTRACT: The decontamination of bisphenol A (BPA) from aqueous solution by graphene adsorption was investigated. The maximum adsorption capacity (q_m) of graphene for BPA obtained from a Langmuir isotherm was 182 mg/g at 302.15 K, which was among the highest values of BPA adsorption compared with other carbonaceous adsorbents according to the literature. Both $\pi-\pi$ interactions and hydrogen bonds might be responsible for the adsorption of BPA on graphene, and the excellent adsorption capacity of graphene was due to its unique sp^2-hybridized single-atom-layer structure. Therefore, graphene could be regarded as a promising adsorbent for BPA removal in water treatment. The kinetics and isotherm data can be well described by the pseudo-second-order kinetic model and the Langmuir isotherm, respectively. The thermodynamic studies indicated that the adsorption reaction was a spontaneous and exothermic process. Besides, the presence of NaCl in the solution could facilitate the adsorption process, whereas the alkaline pH range and higher temperature of the solution were unfavorable.

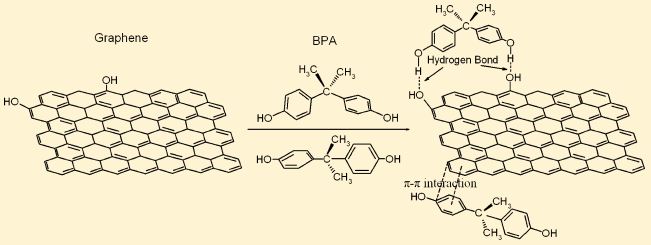

INTRODUCTION

Endocrine-disrupting chemicals (EDCs) can imitate the biological activity of natural hormones, occupy the hormone receptors, or interfere with the transport and metabolic processes of natural hormones, finally pose a risk to animals and humans.[1,2] Hence, EDCs have drawn considerable social and scientific concern in recent years. Bisphenol A (BPA), one of these EDCs, is widely used as a monomer for the production of epoxy resins, polycarbonates, and other plastics. It is considered to be a critical contaminant because its weak estrogen-like effect is harmful to organisms.[3−5] BPA contamination has been reportedly detected in industrial wastewater, groundwater, surface water, and even drinking water.[6−8] Therefore, BPA is selected as the model compound for the removal of water among the EDCs herein.

Nowadays, various removal methods have been used in water treatment, such as adsorption,[9−12] membrane separation,[13] biological treatment,[14] photocatalytic degradation,[15] and other processes. Among these methods, adsorption is a superior and widely used method in terms of its comparatively low cost, ease of operation, and fewer harmful secondary products. Regarding the adsorption technique, the application of effective adsorbents is critical to guaranteeing the efficiency of water treatment. Carbonaceous materials such as activated carbon (AC),[11,16] carbon nanotubes (CNTs),[17] porous carbon,[18] and graphene oxide (GO)[19,20] have always attracted attention because of their chemical stability, large specific surface area, abundant pore size distribution, and feasibility of mass production. Thus, it is important to seek new carbonaceous adsorbents with a high adsorption capacity, fast adsorption rate, and specific surface reactivity.

Graphene, a single atomic layer of sp^2-hybridized carbon arranged in a honeycomb structure, is the 2D allotrope of carbon. It has drawn an enormous amount of scientific attention since its discovery because of its large surface area,[21] extraordinary electronic and mechanical properties,[22] excellent mobility of charge carriers,[23] and good thermal conductivity.[24] Owing to these remarkable properties, graphene is likely to be applied in many fields such as supercapacitors,[25] solar cells,[26] sensors,[27] and adsorbents.[28−31] Recently, it has been reported that graphene shows excellent adsorption capacity for the removal of heavy metal ions (Pb^{2+}, Cd^{2+}, Cr^{6+}, etc.),[30,32] fluoride ions,[28] and dyes (methyl orange, methyl blue, rhodamine B, etc.)[29,31] from aqueous solutions. Compared to other carbonaceous materials, the advantage of graphene is the selective adsorption ability to those aromatic compounds with benzene rings through strong $\pi-\pi$ interaction.[33] Therefore, graphene is expected to be a promising adsorbent for the removal of aromatic compounds in water treatment. However, to our knowledge, no relevant work regarding the application of graphene on BPA removal has been reported.

In this study, the adsorption properties of graphene for the removal of BPA from aqueous solution were investigated under

Received: April 11, 2012
Revised: May 8, 2012
Published: May 9, 2012

different experimental conditions such as the contact time, BPA concentration, temperature, pH, and ionic strength in detail. To evaluate the adsorption capacity further and understand the mechanism of graphene toward BPA, adsorption kinetics, isotherms, and thermodynamic studies have also been estimated from the experimental results.

MATERIALS AND METHODS

Synthesis of Graphene. Graphene oxide (GO) was prepared by the modified Hummers method.[34] Graphite (2.0 g) and $NaNO_3$ (1.0 g) were mixed with 40 mL of H_2SO_4 (98 wt %) in a 500 mL flask and stirred for 30 min in an ice bath. Then $KMnO_4$ (6.0 g) was dropped into the vigorously stirred suspension slowly below 15 °C. The ice bath was then removed, and the mixture was stirred at room temperature until it gradually became a brownish slurry, and then it was diluted slowly with 100 mL of water. The reaction temperature was rapidly increased to 98 °C with effervescence, and the color changed to brown. After that, 200 mL of water and 20 mL of H_2O_2 (30 wt %) were successively added. For purification, the mixture was centrifuged and washed with 10% HCl and then deionized water several times to remove the residual metal ions and acid. After filtration and drying at room temperature, GO was obtained as a powder. Graphene was synthesized by the hydrazine reduction of GO.[35] A 250 mL GO aqueous dispersion (2 mg/mL) was ultrasonicated for 2 h. The solution pH was adjusted to 10.0 by adding a 30% ammonia solution. Then, 5 mL of hydrazine hydrate (80 wt %) was added to the solution at 95 °C and stirred for 5 h. The black solution was filtered, washed thoroughly with deionized water to remove the excess hydrazine, and finally dried at room temperature. The obtained black powder was graphene.

Characterization. The samples were characterized by powder X-ray diffraction (XRD) on a Bruker D8-advance X-ray diffractometer at 40 kV and 40 mA for monochromatized Cu Kα (λ = 1.5406 Å) radiation. The Brunauer–Emmett–Teller (BET) specific surface area of the samples was characterized by nitrogen adsorption at 77 K with a Micromeritics 3020 instrument. Zeta potential measurements were made with a Delsa Nano C zeta potential instrument (Beckman Coulter). AFM images were acquired in phase mode in air using Digital Instruments Shimadzu SPM-9600. (The samples were prepared by drop-casting corresponding dilute dispersions onto a freshly cleaved mica surface.) Fourier transform infrared (FTIR) spectra were recorded on a Thermo Nicolet Avatar 370 spectrometer between 4000 and 400 cm^{-1} using KBr pellets.

Batch Adsorption Experiments. BPA ($((CH_3)_2C(C_6H_4OH)_2$, molecular weight 228.29) was purchased from Beijing Chemical Works, China. BPA was dissolved in ethanol as a stock solution (1000 mg/L) because of its low solubility in water and was further diluted with a large amount of water to the required concentrations before used. All adsorption experiments were performed in sealed 250 mL glass conical bottles that contained 10 mg of graphene and 100 mL of a BPA solution in the appropriate concentration. The bottles were placed in a shaking water bath at a shaking speed of 200 rpm at the appropriate temperature.

An adsorption kinetic study was carried out with an initial BPA concentration of 10 mg/L at 302.15 K, pH 6.0 to determine the minimum time required for adsorption to reach equilibrium. The concentrations of BPA were measured at different time intervals from 0.5 to 10 h.

To evaluate the maximum adsorption capacities and the thermodynamic properties, adsorption isotherms of BPA on graphene were obtained at pH 6.0 at 302.15, 322.15, and 342.15 K, respectively. The initial BPA concentrations ranged from 2 to 50 mg/L.

The effect of pH on the adsorption of BPA was studied with an initial BPA concentration of 10 mg/L in a pH range of 2.0–11.0 at 302.15 K. The solution pH was adjusted with a 0.1 M HCl or NaOH solution.

The effect of the ionic strength on the adsorption of BPA was studied by adding NaCl to 10 mg/L BPA solutions with concentrations ranging from 0.02 to 0.5 M at 302.15 K and pH 6.0.

After adsorption experiments, the suspensions were filtered through 0.45 μm membrane filters. The concentration of BPA was examined by a high-performance liquid chromatography (HPLC, Lumtech) system with a Venusil XBP-C18 column (Agela Technologies Inc.) and a UV absorbance detector (K 2501) operated at 280 nm. The mobile phase was 1.0 mL/min of 70% methanol and 30% deionized water.

RESULTS AND DISCUSSION

Characterization of Graphene. XRD patterns of graphite, GO, and graphene are shown in Supporting Information Figure S1. For graphite, the sharp 002 diffraction peak at 26.4° indicated a highly organized crystal structure, revealing an interlayer spacing of about 0.34 nm. For GO, oxidation treatment caused a decrease in the 002 peak intensity of graphite, and a 001 diffraction peak appeared at 11.0°. This peak demonstrated the typical loose-layer-like structure of GO corresponding to an interlayer spacing of 0.80 nm. For graphene, a weak 002 diffraction peak was shown at 24.0°. The corresponding interlayer spacing was about 0.37 nm, which was slightly larger than that of graphite. It might be due to the residual oxygen-containing groups between the graphene layers that came from the incomplete reduction of GO by hydrazine hydrate. Similar results were also reported in other XRD studies.[36]

The nitrogen adsorption–desorption isotherms are shown in Figure S2. The BET analysis indicated that the specific surface area of graphene was 327 m^2/g. The gap between this obtained value and the theoretical value (2600 m^2/g) of the surface area of graphene might be due to the incomplete exfoliation of GO and the severe aggregation of graphene layers during the reduction process because of the unavoidable van der Waals force between single graphene layers.[29]

The zeta potential is a physical parameter commonly used to quantify the surface electrical potential of the solid particle and the stability of liquid dispersions. The zeta potentials of graphene (Figure S3) measured in aqueous solutions at pH 2.0–11.0 were always negative and decreased with the increase in pH. This indicated that graphene sheets were negatively charged. The zeta potentials were below −30 mV for pH >6.0 and even reached −46 mV for pH 10.0. It is known that zeta potentials lower than −30 mV generally imply sufficient mutual repulsion, which can ensure the stability of a dispersion.[37] Thus, the excellent stability of graphene dispersions could be mainly due to the electrostatic repulsion among graphene sheets.

The morphological structure of graphene was characterized by AFM and is shown in Figure S4. The samples were prepared by casting the graphene dispersion on a freshly cleaved mica surface. The AFM image (Figure S4a) clearly exhibited that graphene sheets were almost transparent with a flakelike shape. The partial overlap of graphene sheets could result in different brightness values on the surface of graphene. The size of the graphene sheets ranged from several tens of nanometers to several micrometers. The cross-section analysis of graphene (Figure S4b) indicated that the average height of graphene sheets was about 0.8 nm, which indicated that graphene existed mainly in a single-layer state in aqueous solution. Similar results had also been observed in other AFM studies.[38]

BPA Adsorption Kinetics. Adsorption kinetics was investigated for a better understanding of the mechanism of adsorption. The effect of contact time on the adsorption of BPA by graphene was studied and shown in Figure 1. It can be seen that the adsorption capacity of graphene increased quickly in the first 0.5 h and then rose slowly until the adsorption

dx.doi.org/10.1021/la301476p | Langmuir 2012, 28, 8418–8425

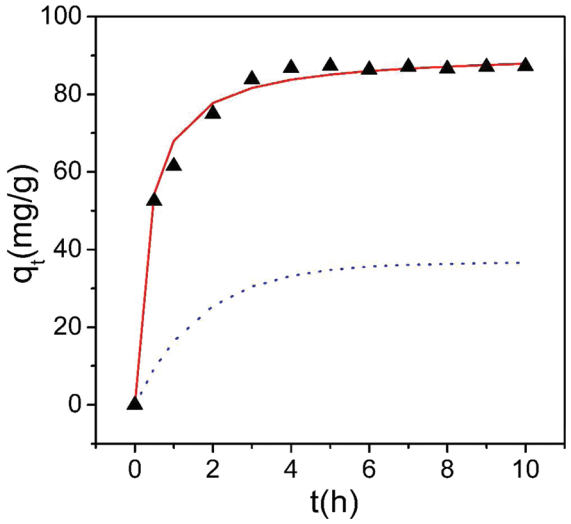

Figure 1. Effect of contact time on the adsorption of BPA by graphene (10 mg of graphene and 100 mL of 10 mg/L BPA at 302.15 K, pH 6.0). The dotted line is the pseudo-first-order model simulation; the solid line is the pseudo-second-order model simulation.

equilibrium was reached within 5 h. On the basis of the above result, a contact time of 6 h was selected for a sure establishment of the adsorption equilibrium in further adsorption studies.

The adsorption capacity of graphene for BPA was calculated according to the following equation

$$q_e = \frac{(C_0 - C_e)V}{m} \quad (1)$$

where C_0 and C_e represent the initial and equilibrium concentrations of BPA aqueous solution (mg/L), V is the volume of the solution (L), and m is the mass of the adsorbent (g).

To investigate the mechanism of the adsorption process, two conventional kinetic models (pseudo-first-order and pseudo-second-order) were applied to analyze the experimental data.

The pseudo-first-order model can be expressed as[39]

$$\ln(q_e - q_t) = \ln q_e - k_1 t \quad (2)$$

where q_e and q_t are the adsorbed BPA amounts on graphene at equilibrium and at various times t (mg/g), respectively, and k_1 is the rate constant of the pseudo-first-order model of adsorption (1/h). The values of q_e and k_1 can be determined from the intercept and slope of the linear plot of $\ln(q_e - q_t)$ versus t.

The pseudo-second-order model includes all the steps of adsorption including external film diffusion, adsorption, and internal particle diffusion, which is described as[40,41]

$$\frac{t}{q_t} = \frac{1}{k_2 q_e^{\,2}} + \frac{t}{q_e} \quad (3)$$

where q_e and q_t are defined as in the pseudo-first-order model and k_2 is the rate constant of the pseudo-second-order model of adsorption (g/mg·h). The slope and intercept of the linear plot of t/q_t against t yield the values of q_e and k_2. Furthermore, the initial adsorption rate h (mg/g·h) can be determined from $h = k_2 q_e^{\,2}$.

The kinetic parameters and correlation coefficients for the removal of BPA by graphene are summarized in Table 1. The correlation coefficient R^2 value for the pseudo-second-order model exceeded 0.99, which was much higher than that of the pseudo-first-order model. Furthermore, the experimental adsorption capacity ($q_{e,exp}$) was also in accordance with the calculated adsorption capacity ($q_{e,cal}$) obtained from the pseudo-second-order model. These results indicated that the pseudo-second-order kinetic model fit the adsorption of BPA on graphene better than did the pseudo-first-order model.

BPA Adsorption Isotherms. The adsorption isotherm models are usually used to indicate the interaction between the absorbent and the adsorbate when the adsorption process reaches equilibrium. Figure 2 shows the adsorption isotherms

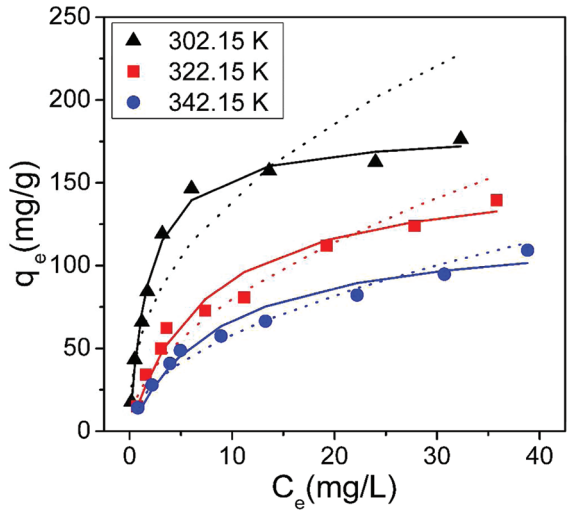

Figure 2. Adsorption isotherms of BPA by graphene at three different temperatures (10 mg of graphene and 100 mL of BPA reacted for 6 h at pH 6.0). The solid lines are the Langmuir model simulation; the dotted lines are the Freundlich model simulation.

of BPA on graphene at three different temperatures. It can be seen that the adsorption capacity of graphene increased with the increasing equilibrium concentration of BPA and reached saturation progressively. This could be due to the increasing driving force of the concentration gradient because the increase in BPA concentration could accelerate the diffusion of BPA molecules onto graphene sheets. The Langmuir and Freundlich isotherm models are the most frequently used.

The Langmuir model assumes that adsorption occurs on a homogeneous surface by monolayer coverage and no subsequent interaction between adsorbed species. The equation is as follows[42]

Table 1. Kinetic Parameters for the Adsorption of BPA by Graphene

	pseudo-first-order			pseudo-second-order			
$q_{e,exp}$ (mg/g)	k_1 (1/h)	$q_{e,cal}$ (mg/g)	R^2	k_2 (g/mg·h)	$q_{e,cal}$ (mg/g)	h (mg/g·h)	R^2
87.30	0.59	36.62	0.8742	0.033	90.74	271.0	0.9991

dx.doi.org/10.1021/la301476p | *Langmuir* 2012, 28, 8418−8425

$$\frac{c_e}{q_e} = \frac{1}{q_m}c_e + \frac{1}{q_m K_L} \quad (4)$$

where q_e is the adsorbed BPA amount per gram of graphene (mg/g), C_e represents the equilibrium concentration of BPA in solution (mg/L), K_L is the Langmuir constant (L/mg), which is related to the affinity of the binding sites, and q_m represents the maximum adsorption capacity of the adsorbent (mg/g). The values of q_m and K_L are calculated from the slope and intercept of the linear plot of C_e/q_e against C_e.

The Freundlich model is an empirical model based on multilayer adsorption on heterogeneous surfaces. The equation is commonly described as[43]

$$\ln q_e = \frac{1}{n}\ln c_e + \ln K_F \quad (5)$$

where q_e and C_e are defined as in the Langmuir isotherm and K_F and n are the Freundlich constants that represent the adsorption capacity and adsorption strength, respectively. The magnitude of $1/n$ quantifies the favorability of adsorption and the degree of heterogeneity of the surface. If $n > 1$, suggesting favorable adsorption, then the adsorption capacity increases and new adsorption sites form.[44] K_F and n can be obtained from the intercept and slope of the linear plot of ln q_e versus ln C_e.

The relative parameters calculated from the Langmuir and Freundlich models at three different temperatures were listed in Table 2. On the basis of a comparison of the correlation coefficient R^2 values, the Langmuir model fitted the adsorption data better than the Freundlich model. In other words, the adsorption of BPA by graphene took place in a monolayer adsorption manner. It can also be seen that q_m calculated from the Langmuir equation decreased with increasing temperature, indicating that adsorption was unfavorable at higher temperature.

Table 2. Isotherm Parameters for the Adsorption of BPA by Graphene

	Langmuir			Freundlich		
T (K)	q_m (mg/g)	K_L (L/mg)	R^2	K_F	n	R^2
302.15	181.82	0.5435	0.9978	54.70	2.436	0.8782
322.15	160.51	0.1334	0.9763	24.39	1.940	0.9306
342.15	123.92	0.1168	0.9733	18.68	2.024	0.9724

In addition, q_m of graphene for BPA at 302.15 K was 182 mg/g, which was among the highest values compared to the values for other carbonaceous adsorbents previously reported in the literature (Table 3).[17,18,45] Considering the BET surface area of the adsorbents, the high affinity of graphene to BPA was even more obvious. Therefore, graphene was an excellent BPA absorbent in wastewater treatment.

Adsorption Thermodynamic Study. The thermodynamic parameters provide in-depth information about internal energy changes that are associated with adsorption. The standard free-energy change ($\Delta G°$), the standard enthalpy change ($\Delta H°$), and the standard entropy change ($\Delta S°$) are calculated from the temperature-dependent adsorption isotherms to predict the adsorption process. The standard free-energy change ($\Delta G°$) can be calculated from the following equation[40]

$$\Delta G° = -RT \ln K° \quad (6)$$

where R is the universal gas constant (8.314 J/mol·K) and T is the absolute temperature (K). The distribution adsorption coefficient, K_d, is calculated from the following equation[40]

$$K_d = \frac{C_0 - C_e}{C_e}\frac{V}{m} \quad (7)$$

where C_0 is the initial concentration (mmol/L), C_e is the equilibration concentration after centrifugation (mmol/L), V is the volume of the suspension (L), and m is the mass of the adsorbent (g). The adsorption equilibrium constant, $K°$, can be calculated by plotting ln K_d versus C_e and extrapolating C_e to zero. The value of the intercept is that of ln $K°$.

The standard enthalpy change ($\Delta H°$) and the standard entropy change ($\Delta S°$) are calculated from the following equation:[40]

$$\ln K° = \frac{\Delta S°}{R} - \frac{\Delta H°}{RT} \quad (8)$$

The slope and intercept of the plot of ln $K°$ versus $1/T$ are $-\Delta H°/R$ and $\Delta S°/R$, respectively.

The thermodynamic parameters calculated from eqs 6−8 at three different temperatures are listed in Table 4. The negative standard free-energy change ($\Delta G°$) indicated that the adsorption was a spontaneous process, and the value of $\Delta G°$ became more negative with the decrease in temperature, indicating that lower temperature facilitated the adsorption of BPA on graphene. The negative $\Delta H°$ value suggested the exothermic nature of adsorption, which was also supported by the decline in the adsorption capacity of BPA with the increase in temperature. Similar results had been published before. The

Table 3. Adsorption Capacity of BPA by Graphene in Comparison to Other Literature Values

adsorbent	pH	T (K)	S_{BET} (m^2/g)	MAC (mg/g)[a]	ref
graphene	6.0	302.15	327	181.6	our study
porous carbon produced at 400 °C from Moso bamboo	NA[b]	296.15	3	2.1	18
porous carbon produced at 700 °C from Moso bamboo	NA[b]	296.15	251	11.4	18
porous carbon produced at 1000 °C from Moso bamboo	NA[b]	296.15	300	41.8	18
AC purchased from Wako	NA[b]	296.15	1350	56.5	18
AC purchased from Takeda	NA[b]	298.15	1119	23.5	45
carbonaceous material produced at 600 °C from wood chips	NA[b]	298.15	NA[b]	4.2−18.2	45
carbonaceous material produced at 800 °C from wood chips	NA[b]	298.15	NA[b]	24.1−31.4	45
as-grown CNTs	6.0	280.15	78	61.0	17
modified CNTs	6.0	280.15	95	70.0	17

[a]Maximum adsorption capacity obtained from the Langmuir model or from the adsorption capacity at the highest initial concentration. [b]Data not available.

dx.doi.org/10.1021/la301476p | Langmuir 2012, 28, 8418−8425

Table 4. Thermodynamic Parameters of BPA Adsorption on Graphene

	T (K)		
thermodynamic constant	302.15	322.15	342.15
ln $K°$	4.105	2.901	2.520
$\Delta G°$ (kJ/mol)	−10.312	−7.770	−7.168
$\Delta H°$ (kJ/mol)		−34.383	
$\Delta S°$ (J/mol·K)		−80.606	

negative standard entropy change ($\Delta S°$) reflected decreased randomness at the solid−liquid interface during the adsorption of BPA on graphene.[17] The values of the thermodynamic parameters gave us insight into the interaction between graphene and BPA.

Effect of the Solution pH and Ionic Strength. The solution pH, which can change the net charge of the adsorbent and adsorbate, is one of the most important factors in determining the adsorption properties of an adsorbent.[28] Figure 3a showed the effect of the solution pH on BPA adsorption by graphene with the initial pH ranging from 2.0 to 11.0. It can be seen that in the acidic pH range from 2.0 to 7.0 the adsorption capacity of graphene showed little change, always remained around 87 mg/g. For pH >7.0, the adsorption capacity declined sharply and even decreased to about 30 mg/g at pH 11.0. These phenomena can be explained by the net charge of graphene and BPA at different pH values. Graphene was always negatively charged over the whole pH scale, as shown in the zeta potential analysis (Figure S3). BPA was in its molecular form at pH <8.0 and started the first deprotonation at around pH 8.0 and the second at around pH 9.0. BPA moleculars were mostly ionized to mono- or divalent anions after the deprotonation.[16] Thus, the reduction of the adsorption capacity of graphene observed in the alkaline pH range might be due to the repulsive electrostatic interactions established between the negatively charged surface of graphene and the bisphenolate anion.

It is well known that industrial sewage contains not only pollutants but also high concentrations of salts, which may affect the removal of pollutants. Therefore, a study was also conducted on the effect of the solution ionic strength on the adsorption of BPA by graphene. As shown in Figure 3b, it can be found that the removal of graphene was improved in the presence of NaCl. When the NaCl concentration was below 0.1 M, the adsorption capacity increased rapidly. This phenomenon can be explained by the negative charge of graphene and the molecular form of BPA at pH 6.0. The ions from NaCl were placed between the surface of graphene and the BPA molecules, which produced a screening effect of the surface charge. It favored adsorbate−adsorbent interactions and enhanced the adsorption of BPA. The presence of NaCl in solution also caused a salting-out effect via decreasing the solubility of BPA, thereby enhancing its adsorption on graphene. The advantageous effect of electrolytes on BPA adsorption was previously reported for AC.[16] However, the adsorption capacity was decreased slightly when the NaCl concentration was >0.1 M. It indicated that NaCl also competed with BPA for the adsorption sites on graphene. The binding sites of graphene available for BPA were now occupied by NaCl.[11]

Adsorption Mechanism. The $\pi-\pi$ interaction has always been applied to explain the mechanism of organic molecules with C═C double bonds or benzene rings adsorbed on the surface of graphene because these organic molecules contain π electrons that interact with the π electrons of benzene rings of graphene by means of $\pi-\pi$ electron coupling.[36] Because BPA also has benzene rings, it could be speculated that the main intermolecular force between BPA and graphene should be the $\pi-\pi$ interaction. Besides, there were some residual oxygen-containing groups such as hydroxyl groups remaining in graphene during the reduction of GO by hydrazine hydrate, which can form hydrogen bonds with hydroxyl groups of BPA. Thus, we can expect that two kinds of adsorbent−adsorbate interactions might be responsible for the adsorption of BPA on graphene.[12] One main interaction was the $\pi-\pi$ interaction between the benzene rings of BPA and the graphene planes. The other was hydrogen bonding between the oxygen-containing groups contained in both BPA and graphene.[46] Figure 4 is the schematic of $\pi-\pi$ interaction and hydrogen bonding between BPA and graphene. To demonstrate the adsorption mechanism further, the FTIR spectra of graphene and graphene after BPA adsorption were compared.

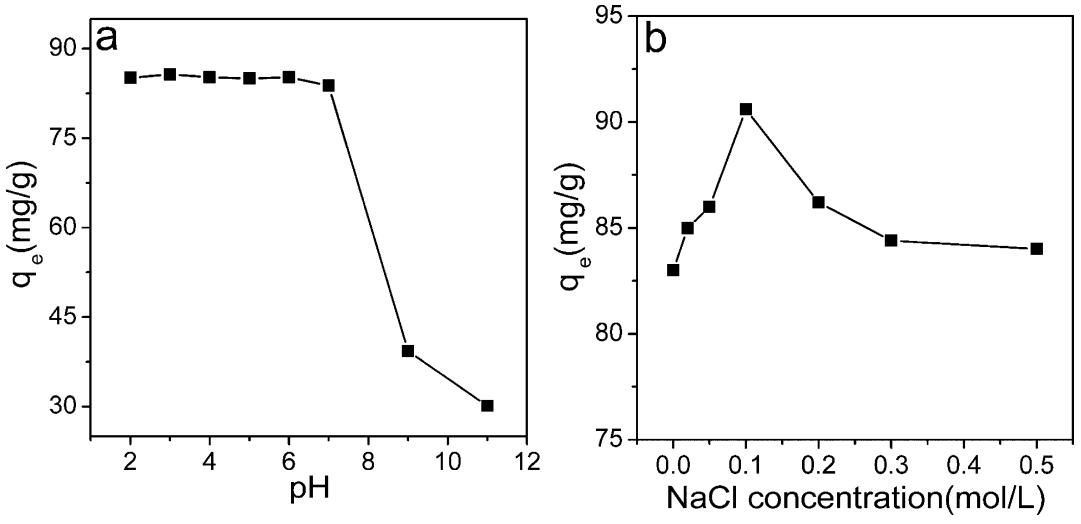

Figure 3. (a) Effect of the solution pH (10 mg of graphene and 100 mL of 10 mg/L BPA reacted for 6 h at 302.15 K). (b) Effect of the ionic strength (10 mg of graphene and 100 mL of 10 mg/L BPA reacted for 6 h at 302.15 K, pH 6.0) on the adsorption of BPA by graphene.

dx.doi.org/10.1021/la301476p | *Langmuir* 2012, 28, 8418−8425

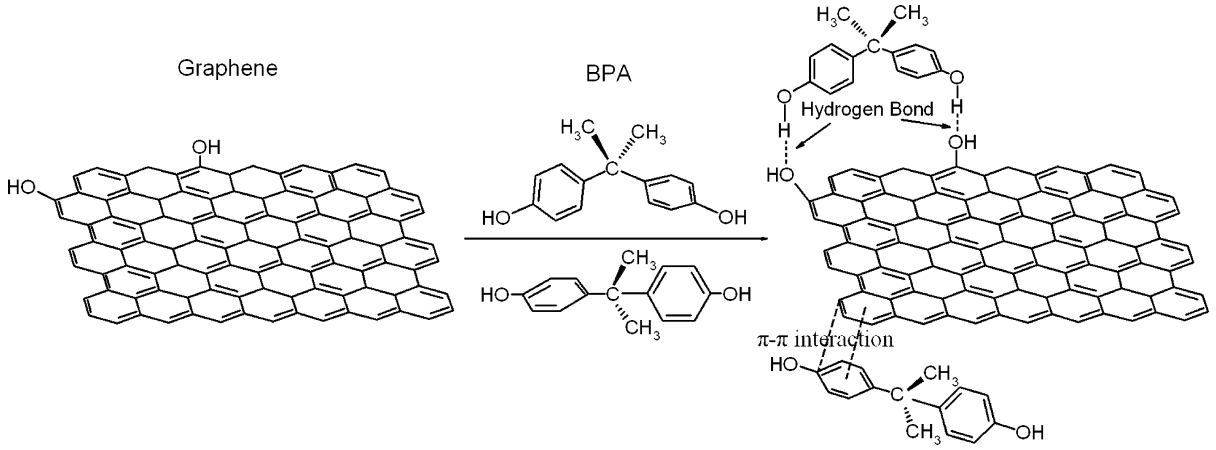

Figure 4. Schematic of $\pi-\pi$ interaction and hydrogen bonding between BPA and graphene.

FTIR spectroscopy is a helpful tool in identifying the presence of certain functional groups on the surface of a solid. The FTIR spectrum of GO was also analyzed and is shown in Figure 5. The strong peak at 3418 cm^{-1} can be attributed to the stretching vibration of O−H groups. The peak at 1727 cm^{-1} was assigned to the appearance of C═O bonds in carboxylic acid and carbonyl moieties. The peak at 1622 cm^{-1} was associated with the skeletal vibration of aromatic C═C bonds. The peak at around 1383 cm^{-1} corresponded to carboxyl O═C−O bonds. The peak at 1223 cm^{-1} referred to epoxy C−O−C bonds. The peak at around 1048 cm^{-1} belonged to alkoxy C−O bonds.[35]

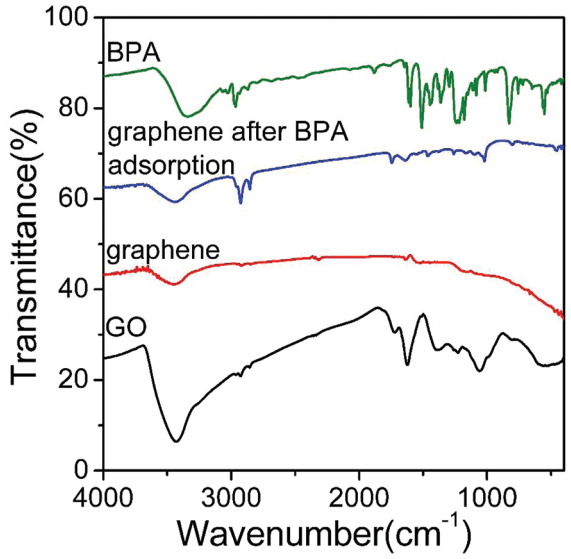

Figure 5. FTIR spectra of GO, graphene, BPA, and graphene after BPA adsorption.

The features in the FTIR spectrum of graphene suggest that most of the oxygen-containing groups had been removed after the reduction of GO by hydrazine hydrate. The peak at 3455 cm^{-1} corresponding to the O−H stretching vibration decreased significantly, and the peaks at 1152 cm^{-1} attributed to the stretching vibration of the C−O bond also became relatively small. The skeletal vibration of aromatic C═C bonds and the C═C stretching vibration were observed at 1633 and 1523 cm^{-1}.[28] Compared to graphene, it can be found that many new peaks were introduced into the FTIR spectrum of graphene after BPA adsorption. These new peaks at 2800−3000 and 400−1800 cm^{-1} were in accordance with the peaks from the FTIR spectrum of BPA and appeared at significant intensities, which indicated that a large number of BPA molecules had been adsorbed on the surface of graphene. Furthermore, the stretching frequency of the O−H group had a small shift from 3455 to 3442 cm^{-1}, which can be ascribed to hydrogen bonding between hydroxyl groups contained in both BPA and graphene.[12] The peak belonging to the skeletal vibration of aromatic C═C bonds also shifted from 1633 to 1641 cm^{-1} and was widened after adsorption, indicating that there might be the $\pi-\pi$ interaction between the benzene rings of BPA and the graphene planes.[47]

Therefore, the result of the FTIR spectroscopy was a new proof in demonstrating the presence of the $\pi-\pi$ interaction and hydrogen bonding between BPA and graphene. Moreover, compared to other carbonaceous materials, graphene has larger and smoother surfaces for forming $\pi-\pi$ interactions that can easily adsorb more organic contaminants.

CONCLUSIONS

Graphene showed excellent adsorption capacity for BPA. The maximum adsorption capacity (q_m) of graphene for BPA obtained from the Langmuir isotherm was 182 mg/g at 302.15 K, which was among the highest values of BPA adsorption compared to that of other carbonaceous adsorbents according to the literature. The influence of the experimental conditions on the adsorption performances of BPA from aqueous solution has been elucidated. The kinetics and isotherm data can be well fitted with the pseudo-second-order kinetic model and the Langmuir isotherm, respectively. The adsorption reaction was a spontaneous exothermic process. Besides, the presence of NaCl in the solution could facilitate the adsorption process, whereas the alkaline pH range and higher temperature of the solution were unfavorable. The large adsorption affinity of graphene for BPA might be due to its single-layer graphene planes with aromatic rings and the residual oxygen-containing groups, which can form $\pi-\pi$ interactions and hydrogen bonds with the benzene rings and hydroxyl groups of BPA. Therefore, graphene is a promising adsorbent for water treatment.

ASSOCIATED CONTENT

Supporting Information

XRD patterns of graphite, GO, and graphene. Nitrogen adsorption−desorption isotherms of graphene. Zeta potential

dx.doi.org/10.1021/la301476p | Langmuir 2012, 28, 8418−8425

analysis of a graphene dispersion. AFM image and cross-sectional analysis of graphene. This material is available free of charge via the Internet at http://pubs.acs.org.

AUTHOR INFORMATION

Corresponding Author

*Tel: +86-10-62787601. Fax: +86-10-62787601. E-mail: zhuyf@mail.tsinghua.edu.cn.

Notes

The authors declare no competing financial interest.

ACKNOWLEDGMENTS

This work was partially supported by the National Natural Science Foundation of China (20925725 and 50972070) and AEMPC201103.

REFERENCES

(1) Ternes, T. A.; Stumpf, M.; Mueller, J.; Haberer, K.; Wilken, R. D.; Servos, M. Behavior and occurrence of estrogens in municipal sewage treatment plants - I. Investigations in Germany, Canada and Brazil. *Sci. Total Environ.* **1999**, *225*, 81−90.

(2) Chang, H. S.; Choo, K. H.; Lee, B.; Choi, S. J. The methods of identification, analysis, and removal of endocrine disrupting compounds (EDCs) in water. *J. Hazard. Mater.* **2009**, *172*, 1−12.

(3) Furhacker, M.; Scharf, S.; Weber, H. Bisphenol A: emissions from point sources. *Chemosphere* **2000**, *41*, 751−756.

(4) Kang, J. H.; Kondo, F.; Katayama, Y. Human exposure to bisphenol A. *Toxicology* **2006**, *226*, 79−89.

(5) Staples, C. A.; Dorn, P. B.; Klecka, G. M.; O'Block, S. T.; Harris, L. R. A review of the environmental fate, effects, and exposures of bisphenol A. *Chemosphere* **1998**, *36*, 2149−2173.

(6) Staples, C. A.; Dorn, P. B.; Klecka, G. M.; O'Block, S. T.; Branson, D. R.; Harris, L. R. Bisphenol A concentrations in receiving waters near US manufacturing and processing facilities. *Chemosphere* **2000**, *40*, 521−525.

(7) Lee, H. B.; Peart, T. E. Bisphenol A contamination in Canadian municipal and industrial wastewater and sludge samples. *Water Qual. Res. J. Canada* **2000**, *35*, 283−298.

(8) Belfroid, A.; van Velzen, M.; van der Horst, B.; Vethaak, D. Occurrence of bisphenol A in surface water and uptake in fish: evaluation of field measurements. *Chemosphere* **2002**, *49*, 97−103.

(9) Pan, B.; Lin, D. H.; Mashayekhi, H.; Xing, B. S. Adsorption and Hysteresis of Bisphenol A and 17 alpha-Ethinyl Estradiol on Carbon Nanomaterials. *Environ. Sci. Technol.* **2009**, *43*, 5480−5485.

(10) Dong, Y.; Wu, D. Y.; Chen, X. C.; Lin, Y. Adsorption of bisphenol A from water by surfactant-modified zeolite. *J. Colloid Interface Sci.* **2010**, *348*, 585−590.

(11) Liu, G. F.; Ma, J.; Li, X. C.; Qin, Q. D. Adsorption of bisphenol A from aqueous solution onto activated carbons with different modification treatments. *J. Hazard. Mater.* **2009**, *164*, 1275−1280.

(12) Kim, Y. H.; Lee, B.; Choo, K. H.; Choi, S. J. Selective adsorption of bisphenol A by organic-inorganic hybrid mesoporous silicas. *Microporous Mesoporous Mater.* **2011**, *138*, 184−190.

(13) Zhang, Y.; Causserand, C.; Aimar, P.; Cravedi, J. P. Removal of bisphenol A by a nanofiltration membrane in view of drinking water production. *Water Res.* **2006**, *40*, 3793−3799.

(14) El-Naas, M. H.; Al-Muhtaseb, S. A.; Makhlouf, S. Biodegradation of phenol by Pseudomonas putida immobilized in polyvinyl alcohol (PVA) gel. *J. Hazard. Mater.* **2009**, *164*, 720−725.

(15) Wang, R.; Ren, D.; Xia, S.; Zhang, Y.; Zhao, J. Photocatalytic degradation of Bisphenol A (BPA) using immobilized TiO_2 and UV illumination in a horizontal circulating bed photocatalytic reactor (HCBPR). *J. Hazard. Mater.* **2009**, *169*, 926−932.

(16) Bautista-Toledo, I.; Ferro-Garcia, M. A.; Rivera-Utrilla, J.; Moreno-Castilla, C.; Vegas Fernandez, F. J. Bisphenol A removal from water by activated carbon. Effects of carbon characteristics and solution chemistry. *Environ. Sci. Technol.* **2005**, *39*, 6246−6250.

(17) Kuo, C. Y. Comparison with as-grown and microwave modified carbon nanotubes to removal aqueous bisphenol A. *Desalination* **2009**, *249*, 976−982.

(18) Asada, T.; Oikawa, K.; Kawata, K.; Ishihara, S.; Iyobe, T.; Yamada, A. Study of removal effect of bisphenol A and beta-estradiol by porous carbon. *J. Health Sci.* **2004**, *50*, 588−593.

(19) Gao, Y.; Li, Y.; Zhang, L.; Huang, H.; Hu, J.; Shah, S. M.; Su, X. Adsorption and removal of tetracycline antibiotics from aqueous solution by graphene oxide. *J. Colloid Interface Sci.* **2012**, *368*, 540−546.

(20) Zhang, W.; Zhou, C.; Zhou, W.; Lei, A.; Zhang, Q.; Wan, Q.; Zou, B. Fast and considerable adsorption of methylene blue dye onto graphene oxide. *Bull. Environ. Contam. Toxicol.* **2011**, *87*, 86−90.

(21) Meyer, J. C.; Geim, A. K.; Katsnelson, M. I.; Novoselov, K. S.; Booth, T. J.; Roth, S. The structure of suspended graphene sheets. *Nature* **2007**, *446*, 60−63.

(22) Lee, C.; Wei, X.; Kysar, J. W.; Hone, J. Measurement of the elastic properties and intrinsic strength of monolayer graphene. *Science* **2008**, *321*, 385−388.

(23) Latil, S.; Henrard, L. Charge carriers in few-layer graphene films. *Phys. Rev. Lett.* **2006**, *97*, 036803.

(24) Balandin, A. A.; Ghosh, S.; Bao, W.; Calizo, I.; Teweldebrhan, D.; Miao, F.; Lau, C. N. Superior thermal conductivity of single-layer graphene. *Nano Lett.* **2008**, *8*, 902−907.

(25) Stoller, M. D.; Park, S.; Zhu, Y.; An, J.; Ruoff, R. S. Graphene-based ultracapacitors. *Nano Lett.* **2008**, *8*, 3498−3502.

(26) Wang, X.; Zhi, L.; Mullen, K. Transparent, conductive graphene electrodes for dye-sensitized solar cells. *Nano Lett.* **2008**, *8*, 323−327.

(27) Ang, P. K.; Chen, W.; Wee, A. T.; Loh, K. P. Solution-gated epitaxial graphene as pH sensor. *J. Am. Chem. Soc.* **2008**, *130*, 14392−14393.

(28) Li, Y.; Zhang, P.; Du, Q.; Peng, X.; Liu, T.; Wang, Z.; Xia, Y.; Zhang, W.; Wang, K.; Zhu, H.; Wu, D. Adsorption of fluoride from aqueous solution by graphene. *J. Colloid Interface Sci.* **2011**, *363*, 348−354.

(29) Liu, T.; Li, Y.; Du, Q.; Sun, J.; Jiao, Y.; Yang, G.; Wang, Z.; Xia, Y.; Zhang, W.; Wang, K.; Zhu, H.; Wu, D. Adsorption of methylene blue from aqueous solution by graphene. *Colloids Surf., B* **2012**, *90*, 197−203.

(30) Deng, X. J.; Lu, L. L.; Li, H. W.; Luo, F. The adsorption properties of Pb(II) and Cd(II) on functionalized graphene prepared by electrolysis method. *J. Hazard. Mater.* **2010**, *183*, 923−930.

(31) Ramesha, G. K.; Kumara, A. V.; Muralidhara, H. B.; Sampath, S. Graphene and graphene oxide as effective adsorbents toward anionic and cationic dyes. *J. Colloid Interface Sci.* **2011**, *361*, 270−277.

(32) Zhu, J.; Wei, S.; Gu, H.; Rapole, S. B.; Wang, Q.; Luo, Z.; Haldolaarachchige, N.; Young, D. P.; Guo, Z. One-pot synthesis of magnetic graphene nanocomposites decorated with core@double-shell nanoparticles for fast chromium removal. *Environ. Sci. Technol.* **2012**, *46*, 977−985.

(33) Cai, X.; Tan, S.; Lin, M.; Xie, A.; Mai, W.; Zhang, X.; Lin, Z.; Wu, T.; Liu, Y. Synergistic antibacterial brilliant blue/reduced graphene oxide/quaternary phosphonium salt composite with excellent water solubility and specific targeting capability. *Langmuir* **2011**, *27*, 7828−7835.

(34) Hummers, W. S.; Offeman, R. E. Preparation of graphitic oxide. *J. Am. Chem. Soc.* **1958**, *80*, 1339−1339.

(35) Chandra, V.; Park, J.; Chun, Y.; Lee, J. W.; Hwang, I. C.; Kim, K. S. Water-dispersible magnetite-reduced graphene oxide composites for arsenic removal. *ACS Nano* **2010**, *4*, 3979−3986.

(36) Wu, T.; Cai, X.; Tan, S.; Li, H.; Liu, J.; Yang, W. Adsorption characteristics of acrylonitrile, p-toluenesulfonic acid, 1-naphthalenesulfonic acid and methyl blue on graphene in aqueous solutions. *Chem. Eng. J.* **2011**, *173*, 144−149.

(37) Everett, D. H. *Basic Principles of Colloid Science*; The Royal Society of Chemistry: London, 1988.

(38) Li, D.; Muller, M. B.; Gilje, S.; Kaner, R. B.; Wallace, G. G. Processable aqueous dispersions of graphene nanosheets. *Nat. Nanotechnol.* **2008**, *3*, 101−105.

(39) Ho, Y. S.; McKay, G. The kinetics of sorption of divalent metal ions onto sphagnum moss flat. *Water Res.* **2000**, *34*, 735−742.
(40) Zhao, G. X.; Li, J. X.; Wang, X. K. Kinetic and thermodynamic study of 1-naphthol adsorption from aqueous solution to sulfonated graphene nanosheets. *Chem. Eng. J.* **2011**, *173*, 185−190.
(41) Blanchard, G.; Maunaye, M.; Martin, G. Removal of heavy-metals from waters by means of natural zeolites. *Water Res.* **1984**, *18*, 1501−1507.
(42) Langmuir, I. The constitution and fundamental properties of solids and liquids. Part I. Solids. *J. Am. Chem. Soc.* **1916**, *38*, 2221−2295.
(43) Freundlich, H. Concerning adsorption in solutions. *J. Phys. Electrochem.* **1906**, *57*, 385−470.
(44) Hameed, B. H. Equilibrium and kinetic studies of methyl violet sorption by agricultural waste. *J. Hazard. Mater.* **2008**, *154*, 204−212.
(45) Nakanishi, A.; Tamai, M.; Kawasaki, N.; Nakamura, T.; Tanada, S. Adsorption characteristics of bisphenol A onto carbonaceous materials produced from wood chips as organic waste. *J. Colloid Interface Sci.* **2002**, *252*, 393−396.
(46) Ersoz, A.; Denizli, A.; Sener, I.; Atilir, A.; Diltemiz, S.; Say, R. Removal of phenolic compounds with nitrophenol-imprinted polymer based on pi-pi and hydrogen-bonding interactions. *Sep. Purif. Technol.* **2004**, *38*, 173−179.
(47) Coughlin, R. W.; Ezra, F. S. Role of surface acidity in the adsorption of organic pollutants on the surface of carbon. *Environ. Sci. Technol.* **1968**, *2*, 291−297.